

Chapter 5

f-family orbits of Sun-Saturn system in elliptical restricted three body problem

5.1 Introduction

A particular family of planar periodic orbits encompassing the second primary was introduced by Broucke in 1968 (Broucke (1968)) and he denoted this family as “C”-family. Later, Hénon denoted this family as *f*-family. The members of this family are stable retrograde planar orbits surrounding Lagrangian points L_1 and L_2 . These orbits are also Distant Retrograde Orbits (DROs). Since *f*-family orbits are highly stable, a spacecraft placed in this orbit requires less fuel. In solar system, some asteroids are in *f*-family orbits with one of the planets. The asteroid 2002VE68 is in a *f*-family orbit around the Sun-Venus system (Sidorenko (2014)). The spacecraft Orion of NASA’s Artemis 1 mission is placed in a DRO around the Moon. So, it can spend more time in deep space with less fuel and can ensure spacecraft systems like guidance, navigation, communication, power and thermal control for future crewed missions (<https://rb.gy/4a681>).

In the Earth-Moon CRTBP, the effects of Jacobi constant on parameters of *f*-family orbits has been studied by Zimovan (2017) using the numerical technique of pseudo-arclength continuation. The method of PSS can also be applied for identifying the location of *f*-family orbits and studying the effects of perturbations on parameters of these orbits. Many researchers (Dutt and Sharma (2010), Dutt and Sharma (2011a), Dutt and Sharma (2011b), Safiya Beevi and Sharma (2011), Safiya Beevi and Sharma (2012b), Safiya Beevi and Sharma (2012a), and Pathak and Thomas (2016)) have used

the method of PSS for finding *f*-family as well as various planar periodic orbits in different systems. The system of equations representing the motion of infinitesimal body as described in Szebehely (1967) is a non-autonomous system due to which Jacobi integral does not exist in ERTBP. So, the computation of periodic orbits in ERTBP using PSS technique is seldom found in literature. To convert this non-autonomous system into an autonomous system, Singh and Umar (2012a) considered eccentric anomaly as independent variable and averaged the system with respect to new independent variable. In this revised representation of equations of motion, the integral of motion, known as energy constant or Jacobi constant, exists in ERTBP, which is the most useful characteristic. Hence, this technique has been used by researchers (Singh and Umar (2012b), Chakraborty and Narayan (2018), Singh and Isah (2021), and Sheth and Thomas (2022)) for the study of ERTBP.

In this chapter, using equations (1.49), the technique of PSS has been extended from CRTBP to ERTBP and *f*-family orbits in the Sun-Saturn system with the Sun as a source of radiation are computed. The PSS are plotted for different values of eccentricity of primaries' orbit and radiation pressure. From these plots of PSS, islands containing *f*-family orbits are identified and the effects of eccentricity, solar radiation and Jacobi constant on *f*-family orbits and their parameters are examined. Further, with the help of regression analysis, estimator functions for parameters of *f*-family orbits are obtained by considering the eccentricity of the orbit of the primaries' as independent variable.

5.2 Existence of Jacobi constant

Multiplying the first equation of system (1.49) by x' and the second equation of system (1.49) by y' , we get,

$$\begin{aligned} x'x'' - 2x'y' &= x' \frac{\partial \bar{\Omega}}{\partial x}, \\ y'y'' + 2x'y' &= y' \frac{\partial \bar{\Omega}}{\partial y}. \end{aligned} \tag{5.1}$$

Adding above equations and integrating with respect to E , we get

$$\int (x'x'' + y'y'') dE = \int \left(x' \frac{\partial \bar{\Omega}}{\partial x} + y' \frac{\partial \bar{\Omega}}{\partial y} \right) dE = \int \left(\frac{\partial \bar{\Omega}}{\partial x} dx + \frac{\partial \bar{\Omega}}{\partial y} dy \right) = \int d\bar{\Omega} \tag{5.2}$$

which gives

$$x'^2 + y'^2 = 2\bar{\Omega} - C, \tag{5.3}$$

where C is a constant of integration. It is known as Jacobian constant or energy constant.

The relation between the eccentric anomaly (E) and time can be obtained using the Kepler's equation for elliptic orbits given by (Danby (1962, p.133))

$$M = E - e \sin(E), \quad (5.4)$$

where M is called the mean anomaly and it is defined as $M = nt$ (Danby (1962, p.132)) in which n is mean motion and t is time. Since we have considered dimensionless synodic coordinate system and primaries are perfect spheres, the value of mean motion n is 1. Using equation (5.4) and the expression for M , we get,

$$t = M = E - e \sin(E). \quad (5.5)$$

Equation (5.5) can be used to convert eccentric anomaly to time.

5.3 Regression Analysis

Regression analysis is a statistical method which is commonly used for finding the functional relationships among variables. This relationship is expressed in the form of an equation or a model which connects the dependent and independent variables. There can be one or more independent variables which are commonly known as predictor variables and the dependent variable is known as the response variable.

Let Y be a response variable and X_1, X_2, \dots, X_p be predictor variables. Then the relationship between Y and X_1, X_2, \dots, X_p can be approximated by the regression model

$$Y = f(X_1, X_2, \dots, X_p) + \varepsilon,$$

where ε denotes a random error which represents the failure of the model to fit the data exactly. The function $f(X_1, X_2, \dots, X_p)$ can be a polynomial or any transcendental function which describes the relationship between Y and X_1, X_2, \dots, X_p .

5.4 Results and Discussion

The mass factor of the Sun-Saturn system is $\mu = 2.857696 \times 10^{-6}$. In this system, the PSS for different values of $e \in [0.0, 0.1]$ and $q \in [0.98, 1.00]$ are plotted. For getting PSS, the value of Jacobi constant is selected and then RKG method is applied to the first order system corresponding to system (1.49) with fixed step size 0.001. Here,

initial state vector for RKG method is of the form $[x_0 \ 0 \ 0 \ y'_0]$, where $x_0 \in [0.4, 1.0]$ and y'_0 can be calculated from equation (1.52). The value of Jacobi constant is constrained by the integral of motion, equation (5.3). If the value of C is selected at random, then the velocity of infinitesimal body might be a complex number. Using equation (1.52) and a fixed pair (q, e) , the maximum value of C , say C_M , can be obtained such that for $C \geq C_M$, the velocity might be complex in some region. The region where the velocity becomes complex is called excluded region as spacecraft cannot travel in that region.

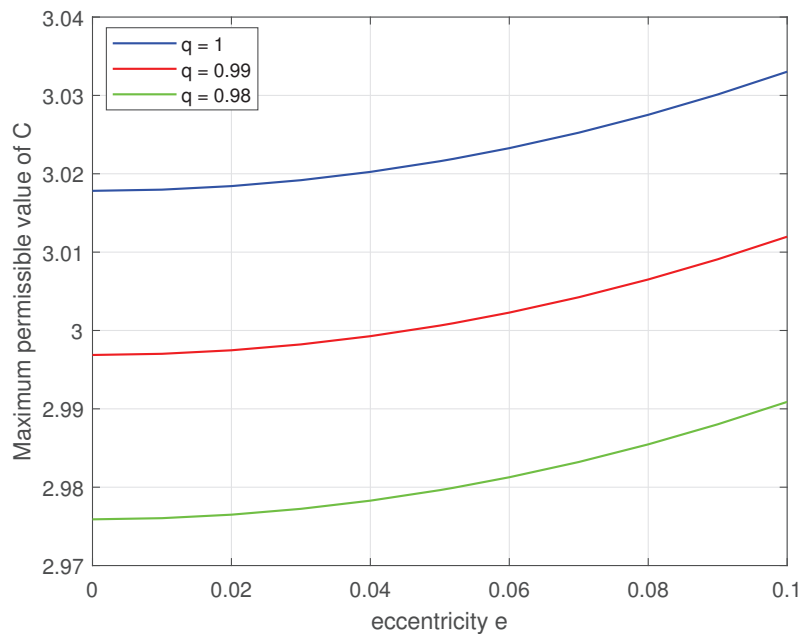


FIGURE 5.1: Maximum permissible value of energy constant against eccentricity

In Fig. 5.1, the variation in the value of C_M due to variation in the eccentricity of the primaries' orbit (e) and mass reduction factor (q) is shown graphically. With the increase in the value of e , the value of C_M also increases. Further, C_M is a non-linear function of e (Fig. 5.1). With the use of MATLAB, a curve is fitted for estimating the functional relation between C_M and e by using regression analysis. Suppose \hat{C}_M denotes the predicted function for C_M . Then a quadratic polynomial in e turns out to be of the best fit for all three values of q . This estimated functional relation between C_M and e is given by

$$\hat{C}_M = \begin{cases} 1.529 e^2 - 0.0010270 e + 3.01783, & q = 1.00; \\ 1.518 e^2 - 0.0010140 e + 2.99688, & q = 0.99; \\ 1.508 e^2 - 0.0009935 e + 2.97591, & q = 0.98. \end{cases}$$

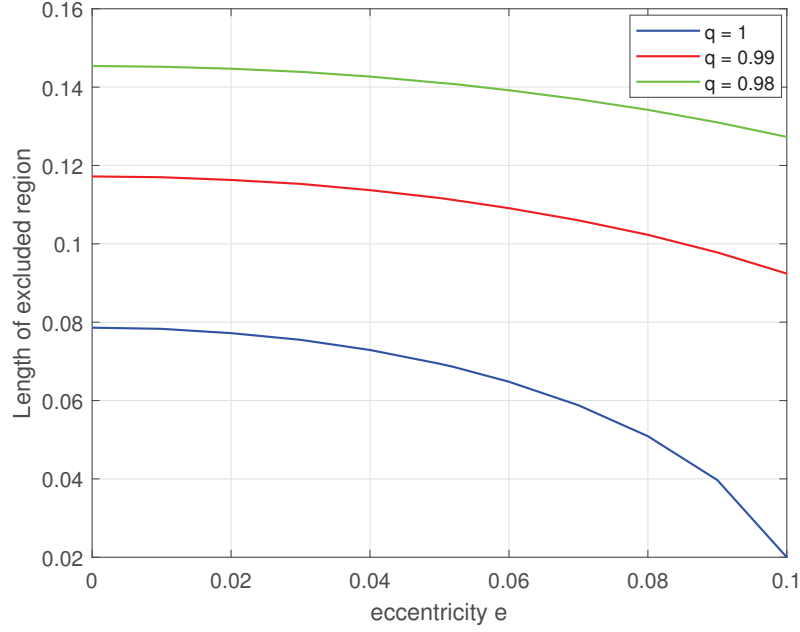


FIGURE 5.2: Length of excluded region against eccentricity

The length of excluded region (L) for $C = 3.014$ is plotted in Fig. 5.2 for values of e in the interval $[0.0, 0.1]$. It can be clearly observed from the Fig. 5.2 that the length of excluded region decreases with the increase in the eccentricity of primaries' orbit which means the permissible region of motion for a spacecraft expands. Also, the functional relation between e and L is non-linear. For $C \geq C_M$, the location and length of excluded region for values of e are given in Table 5.1. In this table, x_l and x_u , respectively, denotes the lower and upper bound of excluded region and L denotes the length of excluded region which is computed using $L = x_u - x_l$. From Table 5.1, it can be observed that as the value of C increases, excluded region expands while the reverse effect is observed due to increase in e . Also, the excluded region shifts towards the Saturn as the eccentricity of orbit of primaries increases. The estimator for the length of excluded region, \hat{L} , is given by

$$\hat{L} = \begin{cases} \begin{bmatrix} -1.911 \times 10^8 e^8 + 6.883 \times 10^7 e^7 - 1.033 \times 10^7 e^6 \\ + 8.284 \times 10^5 e^5 - 3.811 \times 10^4 e^4 + 982.7 e^3 - 16.38 e^2 \\ + 0.06613 e + 0.0786 \end{bmatrix}, & q = 1.00; \\ \begin{bmatrix} -2.16 \times 10^7 e^8 + 1.039 \times 10^7 e^7 - 2.038 \times 10^6 e^6 \\ + 2.08 \times 10^5 e^5 - 1.177 \times 10^4 e^4 + 359 e^3 - 7.456 e^2 \\ + 0.02808 e + 0.1172 \end{bmatrix}, & q = 0.99; \\ \begin{bmatrix} 8.011 \times 10^5 e^7 - 2.647 \times 10^5 e^6 + 3.298 \times 10^4 e^5 \\ - 1908 e^4 + 47.21 e^3 - 1.938 e^2 - 0.004027 e + 0.1454 \end{bmatrix}, & q = 0.98. \end{cases}$$

TABLE 5.1: Excluded region for $C > C_M$ when $q = 1$

e	C	x_l	x_u	L
0	3.018	0.9503	0.9589	0.0086
	3.019	0.9428	0.9649	0.0221
	3.020	0.9382	0.9681	0.0299
	3.021	0.9344	0.9704	0.0360
0.01	3.018	0.9531	0.9564	0.0033
	3.019	0.9437	0.9643	0.0206
	3.020	0.9388	0.9677	0.0289
	3.021	0.9349	0.9701	0.0352
0.02	3.019	0.9466	0.9620	0.0154
	3.020	0.9408	0.9663	0.0255
	3.021	0.9366	0.9691	0.0325
	3.022	0.9330	0.9712	0.0382
0.03	3.020	0.9449	0.9634	0.0184
	3.021	0.9397	0.9671	0.0274
	3.022	0.9357	0.9697	0.0340
	3.023	0.9322	0.9717	0.0394
0.04	3.021	0.9453	0.9631	0.0178
	3.022	0.9400	0.9669	0.0269
	3.023	0.9359	0.9695	0.0336
	3.024	0.9324	0.9716	0.0391

In this case, the eighth degree polynomial in e gives the best approximation for $q = 1.00$ and $q = 0.99$ while for $q = 0.98$, a polynomial of degree seven gives the best approximation.

5.4.1 Effects of eccentricity of primaries' orbit

The eccentricity of the primaries' orbit determines the location of *f*-family orbits. In Fig. 5.3, location of these orbits for three different values of q and C are shown corresponding to different values of e in the range $[0.0, 0.1]$. It can be observed from Figs. 5.3(A), 5.3(B) and 5.3(C) that the orbits shift towards the first primary P_1 with the increase in e . Further, there is a non-linear relation between the location of orbits and eccentricity of primaries' orbit which depends on the values of q as well

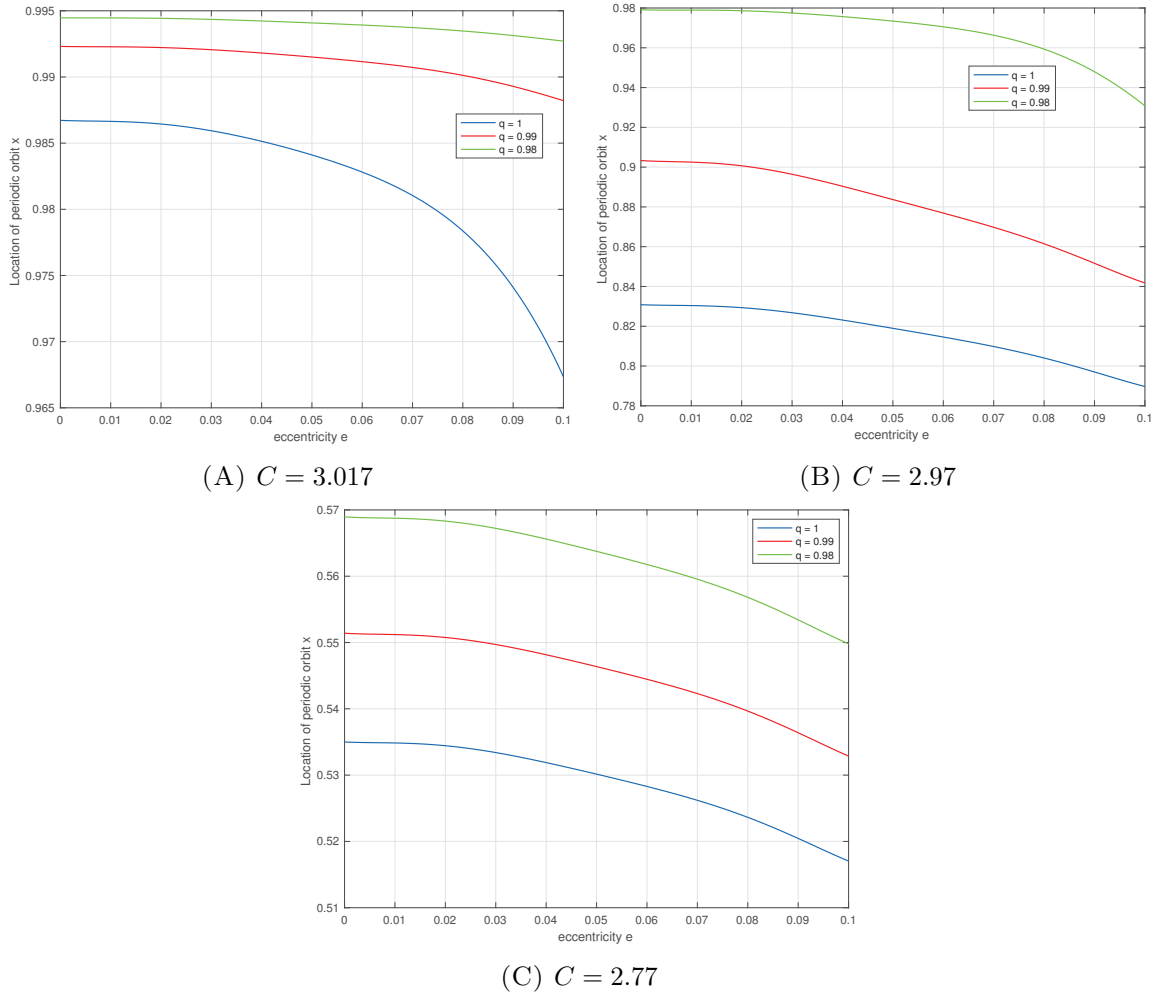


FIGURE 5.3: Variation in location of periodic orbits due to variation in radiation pressure

as C . Suppose \hat{x} denotes the estimator of location of orbits. Then for $C = 3.017$, a biquadratic polynomial in e provides the best estimate for the location (x) of periodic orbits for $q = 1.00, 0.99$ and 0.98 . This estimator function is given by

$$\hat{x} = \begin{cases} -555.6 e^4 + 74.98 e^3 - 4.368 e^2 + 0.05 e + 0.9867, & q = 1.00; \\ -56.07 e^4 + 7.507 e^3 - 0.6539 e^2 + 0.00547 e + 0.9923, & q = 0.99; \\ -20.19 e^4 + 3.012 e^3 - 0.3016 e^2 + 0.002639 e + 0.9945, & q = 0.98. \end{cases}$$

From Fig. 5.3(A), it can be observed that with the increase in the eccentricity of the primaries' orbit, the rate of change in the location of f -family orbit increases and it is highest for $q = 1$.

TABLE 5.2: Initial conditions for f -family orbits

C	e	q	x_0	q	x_0	q	x_0
	0.000		0.986722		0.99231		0.99447
	0.010		0.986645		0.99228		0.99446
	0.030		0.985936		0.99206		0.99435
3.017	0.052	1	0.984107	0.99	0.99151	0.98	0.99409
	0.070		0.981043		0.99072		0.99373
	0.090		0.974100		0.98929		0.99313
	0.100		0.967341		0.98821		0.99271
	0.000		0.83084		0.90330		0.97910
	0.010		0.83039		0.90252		0.97894
	0.030		0.82680		0.89640		0.97750
2.970	0.052	1	0.81895	0.99	0.88370	0.98	0.97342
	0.070		0.80980		0.86975		0.96632
	0.090		0.79700		0.85164		0.94794
	0.100		0.78970		0.84175		0.93080
	0.000		0.53500		0.55140		0.56895
	0.010		0.53485		0.55120		0.56875
	0.030		0.53300		0.54640		0.56722
2.770	0.052	1	0.53015	0.99	0.54637	0.98	0.56375
	0.070		0.52620		0.54230		0.55955
	0.090		0.52045		0.53639		0.55342
	0.100		0.51702		0.53287		0.54980

In Table 5.2, the x -coordinates (x_0) of periodic orbits at initial time are listed for three different values of q and C . Since the initial state vector of f -family orbits is of the form $[x_0 \ 0 \ 0 \ y'_0]$ and y'_0 can be obtained from equation (1.52), the state vector at initial time can be obtained with the help of x_0 . The values x_0 denote the centre of islands, where the periodic orbits lie. These values can be determined from the plots of PSS. From Table 5.2 also it can be analyzed that orbits shift towards the Sun with the increase in the value of e . Also, the rate of change in the location depends on the values of mass reduction factor and Jacobi constant.

The diameter of an orbit is the distance between the two points where the orbit intersects the x -axis. In Fig. 5.4, the variations in diameter of f -family orbits corresponding to different values of e in the interval $[0.0, 0.1]$ for $C = 3.017, 2.97$ and 2.77 are shown

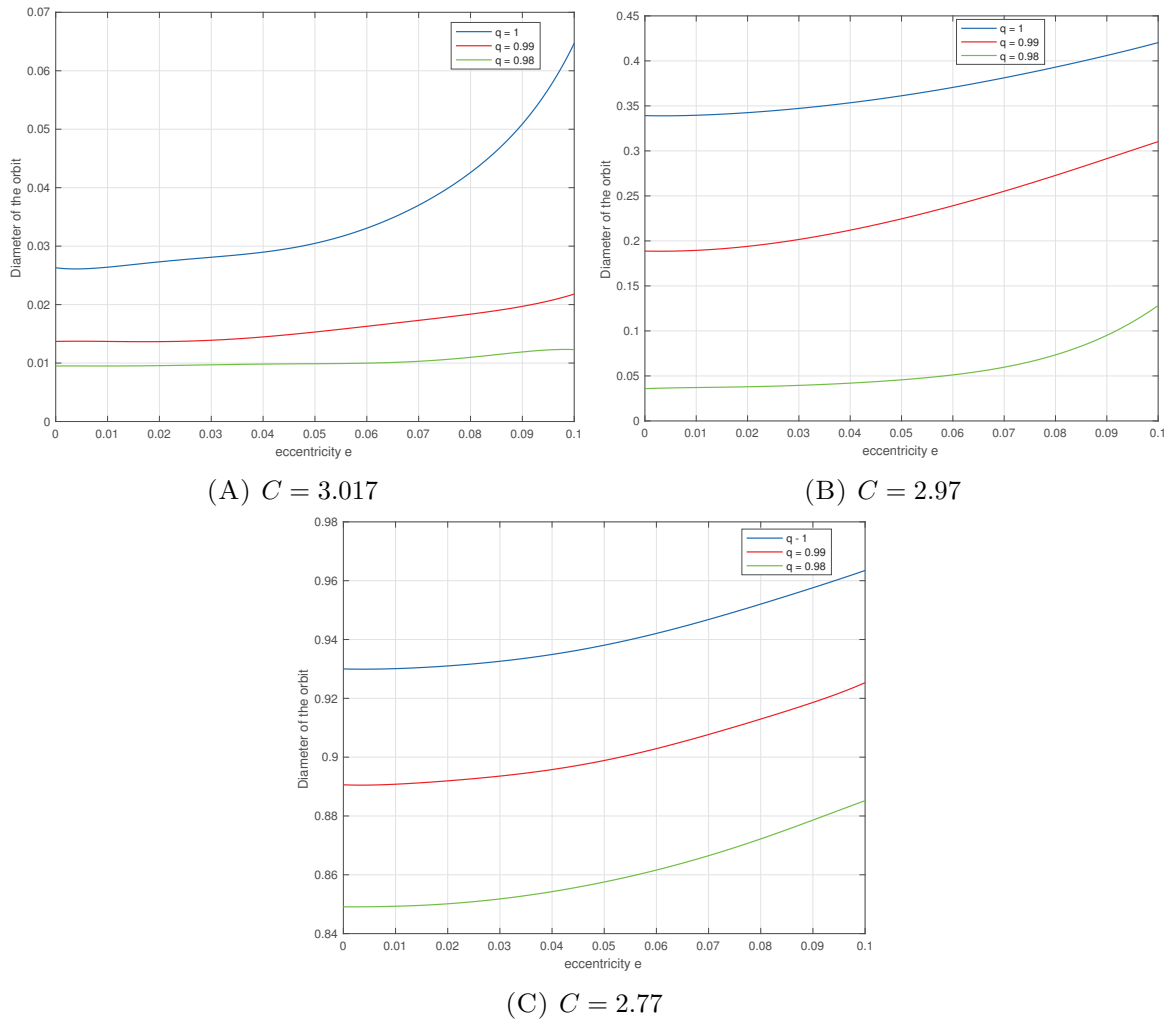


FIGURE 5.4: Variation in diameter of periodic orbits due to variation in radiation pressure

graphically. The diameter of orbit is a monotonically increasing function of eccentricity. From Figs. 5.4(A), 5.4(B) and 5.4(C), it can be observed that the functional relation between diameter of orbit and eccentricity depends on the value of the radiation pressure of the Sun and Jacobi constant. The increase in the value of the diameter of the orbits represents that orbits expand in size as the value of e increases. This variation in size of orbits for $C = 3.017$ and $q = 1$ corresponding to six distinct values of e are shown in Fig. 5.5. The Lagrangian points L_1 and L_2 always lie inside f -family orbits but the barycentre of the primaries never lies inside the orbits even though orbits expand.

The diameter of f -family orbits can be estimated by a biquadratic polynomial in e when the perturbation due to solar radiation is neglected while for $q = 0.99$ and 0.98 , a quintic in e provides the best approximation. The approximator function, \hat{d} , for

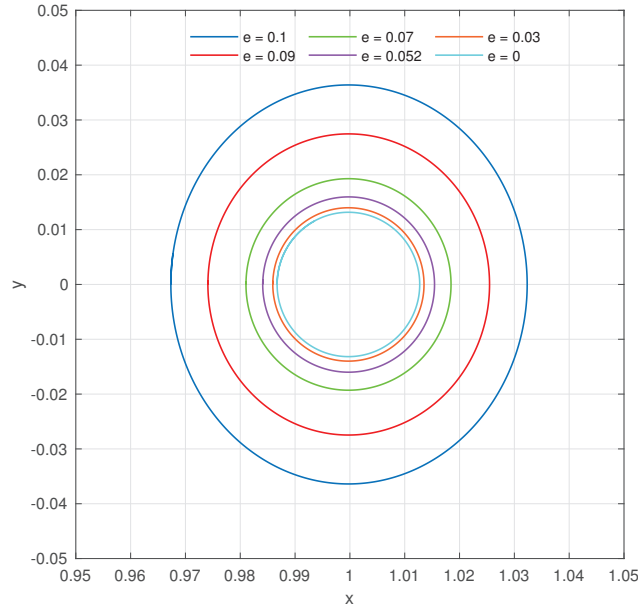


FIGURE 5.5: Variation in shape and size of orbits due to variation in eccentricity for $C = 3.017$ and $q = 1$

diameter of orbits corresponding to $C = 2.97$ (Fig. 5.4(B)) is given by

$$\hat{d} = \begin{cases} 189.3 e^4 - 57.1 e^3 + 12.61 e^2 - 0.06764e + 0.3392, & q = 1.00; \\ -4144 e^5 + 1089 e^4 - 161.3 e^3 + 22.92 e^2 - 0.1375 e + 0.1887, & q = 0.99; \\ 17750 e^5 - 2436 e^4 + 190.8 e^3 - 4.661 e^2 + 0.1419 e + 0.03592, & q = 0.98. \end{cases}$$

The left and the right end points of the island are called the left and the right tips, respectively, and they are denoted by x_L and x_R . An orbit which has initial x -coordinate, x_0 , between x_L and x_R , that is, an orbit with $x_0 \in [x_L, x_R]$ will be periodic or quasi periodic. If $x_0 < x_L$ or $x_0 > x_R$, then orbit will be chaotic; hence the region between x_L and x_R is called the stability region for f -family orbits. The length of the island or stability region is called the amplitude A and it is defined as $A = x_R - x_L$. The values of x_L and x_R can be noted from the plots of PSS. If the amplitude of the island is zero, then a small deviation in the initial condition of f -family orbit gives a chaotic orbit. In this case, the stability of f -family orbit becomes zero. For non-zero values of A , a small deviation in f -family orbit will give a quasi periodic orbit. The locations of left and right tips of islands for $e = 0.00$ and $e = 0.09$ are shown in Fig. 5.6. In Fig. 5.6(A) and 5.6(B), locations of tips of islands corresponding to different values of C are plotted for $e = 0.00$ and $e = 0.09$, respectively, by taking $q = 1$. By considering $q = 0.98$, locations of tips, x_L and x_R , of islands are plotted for $e = 0.00$ and $e = 0.09$ in Fig. 5.6(C) and Fig. 5.6(D), respectively. PSS were plotted for different values of C and from these plots, the values of tips, x_L and x_R , were noted. In Fig. 5.6, left

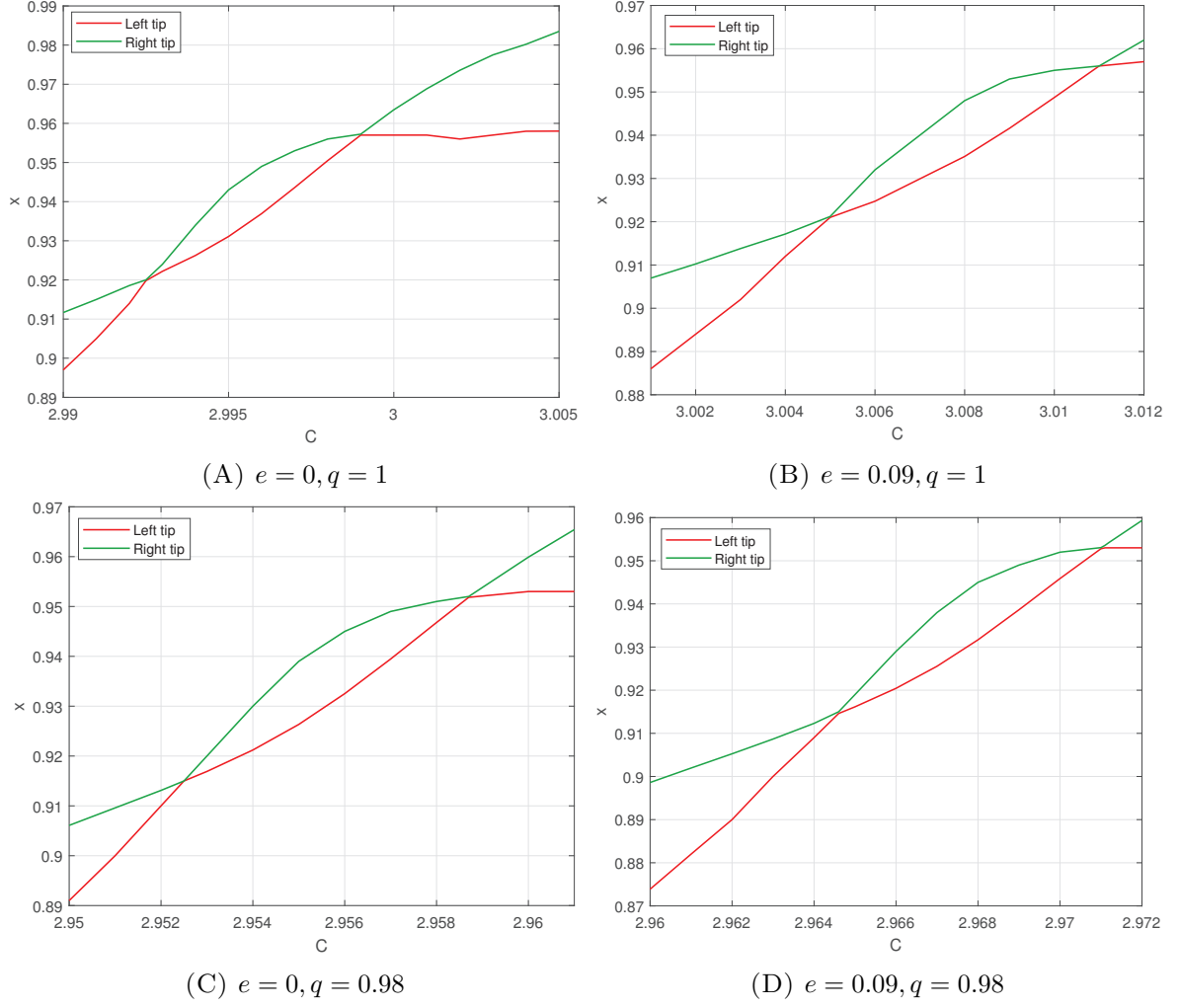


FIGURE 5.6: Stability of f -family orbits

tips x_L are denoted by red colour and right tips x_R are denoted by green colour. The locations at which x_L and x_R have equal values are called separatrices and the stability of f -family orbits become zero at such locations. In Pathak and Thomas (2016), the authors have shown that f -family orbits have two separatrices in CRTBP. From Fig. 5.6, it can be observed that for two different values of C , the values of x_L and x_R are equal in each case which shows that in ERTBP framework also, f -family orbits have two separatrices. In Fig. 5.6(A), the first separatrix occurs at $C_1 = 2.9927$ and the second separatrix occurs at $C_2 = 2.9989$. So, the difference between the energy levels at separatrices is $C_2 - C_1 = 0.0062$. In Fig. 5.6(B), $C_1 = 3.0049$ and $C_2 = 3.0111$ so, $C_2 - C_1 = 0.0062$, and $C_1 = 2.9525$, $C_2 = 2.9588$ and $C_2 - C_1 = 0.0063$ in Fig. 5.6(C) while $C_1 = 2.9644$, $C_2 = 2.97102$ and $C_2 - C_1 = 0.00662$ in Fig. 5.6(D). Thus, in the absence of radiation pressure, the difference between the energy levels at separatrices is same for all values of e while it depends on the value of e in the presence of radiation pressure. It can be observed from Fig. 5.6 that as e increases, the energy level at which

the separatrix occurs also increases.

Islands of PSS containing the centre of *f*-family orbits for different *C* with $e = 0.09$ and $q = 1$ are shown in Fig. 5.7. The direction of islands before and after occurrence of separatrices are shown in this figure. Fig. 5.7(B) corresponds to $C = 3.0049$ where the first separatrix occurs. The amplitude of island is very less for the values of *C* in the neighborhood of $C = 3.0049$. At $C = 3.0049$, the island disappears. The direction of the island changes after the occurrence of a separatrix.

In Fig. 5.8, changes in the period of periodic orbits due to changes in the values of e and q are shown for $C = 3.017, 2.97$ and 2.77 . It can be clearly noted that period is a monotonically increasing function of e (Fig. 5.8). Further, this relation depends on the value of radiation pressure and energy level also.

5.4.2 Effects of radiation pressure

The variation in the value of C_M and the length of excluded region due to radiation of the Sun is shown in Fig. 5.1 and Fig. 5.2, respectively. In both the figures, the curves in blue, red and green correspond to $q = 1.00, 0.99$ and 0.98 , respectively. With the increase in the value of solar radiation, the value of C_M decreases (Fig. 5.1). From Fig. 5.2, it can be observed that with the increase in solar radiation, the length of excluded region increases which shows that the permissible region of motion for a spacecraft decreases due to increase in solar radiation. In Fig. 5.2, the lengths of excluded region are plotted for $C = 3.034$.

In Fig. 5.3, the variation in location of periodic orbits for different values of mass reduction factor is shown. Blue curves correspond to $q = 1$ and red, green curves correspond to $q = 0.99, 0.98$, respectively. Fig. 5.3(A) shows that for $e \geq 0.045$, the rate of change in location of orbits increases and orbits rapidly move towards the more massive primary when $q = 1$ which is not the case for $q = 0.99$ and $q = 0.98$. For $C = 2.97$ (Fig. 5.3(B)), a rapid change in location of orbits is observed for $q = 0.98$. In this case, the estimators are

$$\hat{x} = \begin{cases} -255.4 e^4 + 57.6 e^3 - 7.796 e^2 + 0.04755 e + 0.8308, & q = 1.00; \\ -441.5 e^4 + 112 e^3 - 13.78 e^2 + 0.08391 e + 0.9032, & q = 0.99; \\ -1308 e^4 + 161.9 e^3 - 8.889 e^2 + 0.09614 e + 0.979, & q = 0.98. \end{cases}$$

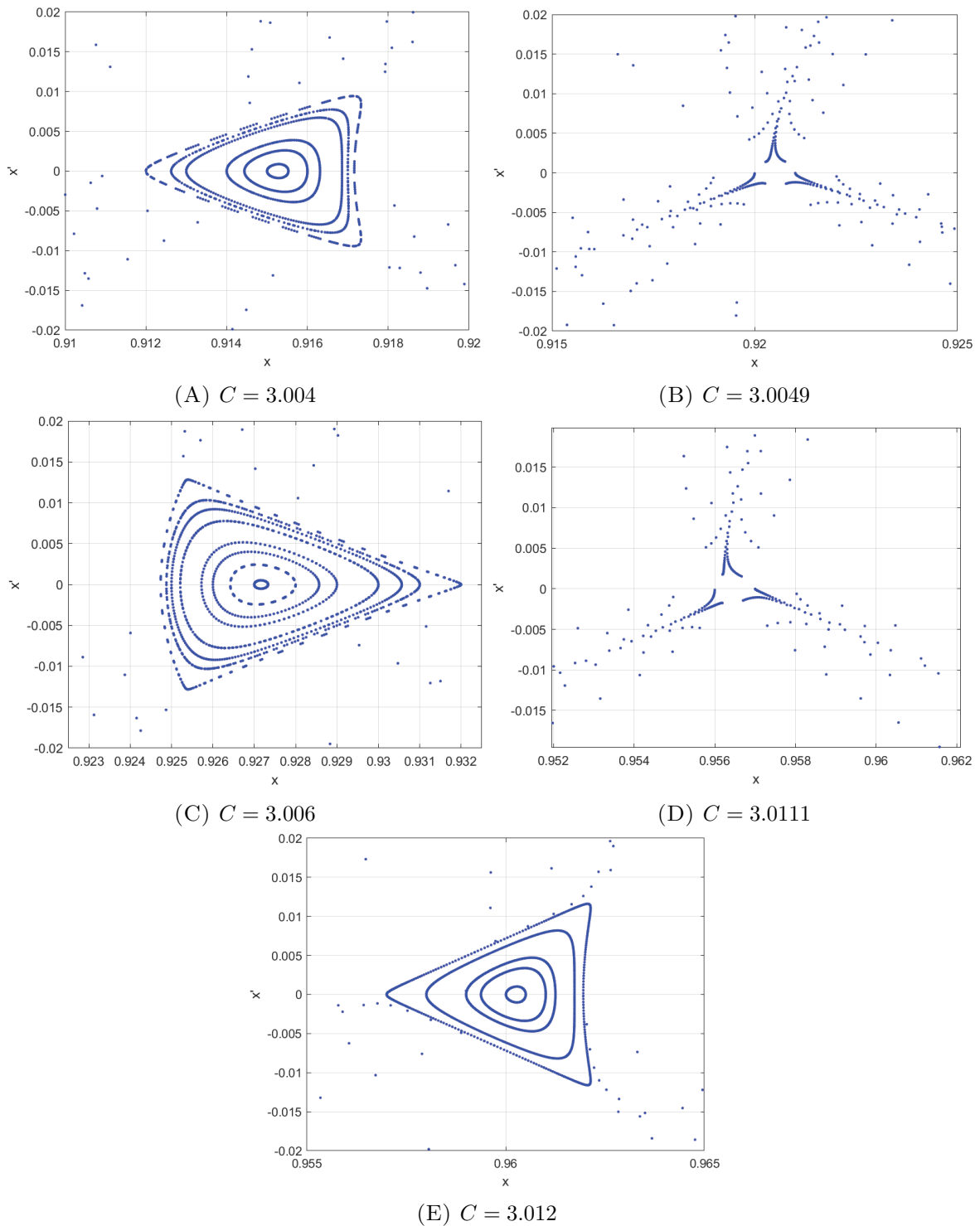


FIGURE 5.7: Variation in shape and size of islands due to variation in C for $e = 0.09$ and $q = 1$

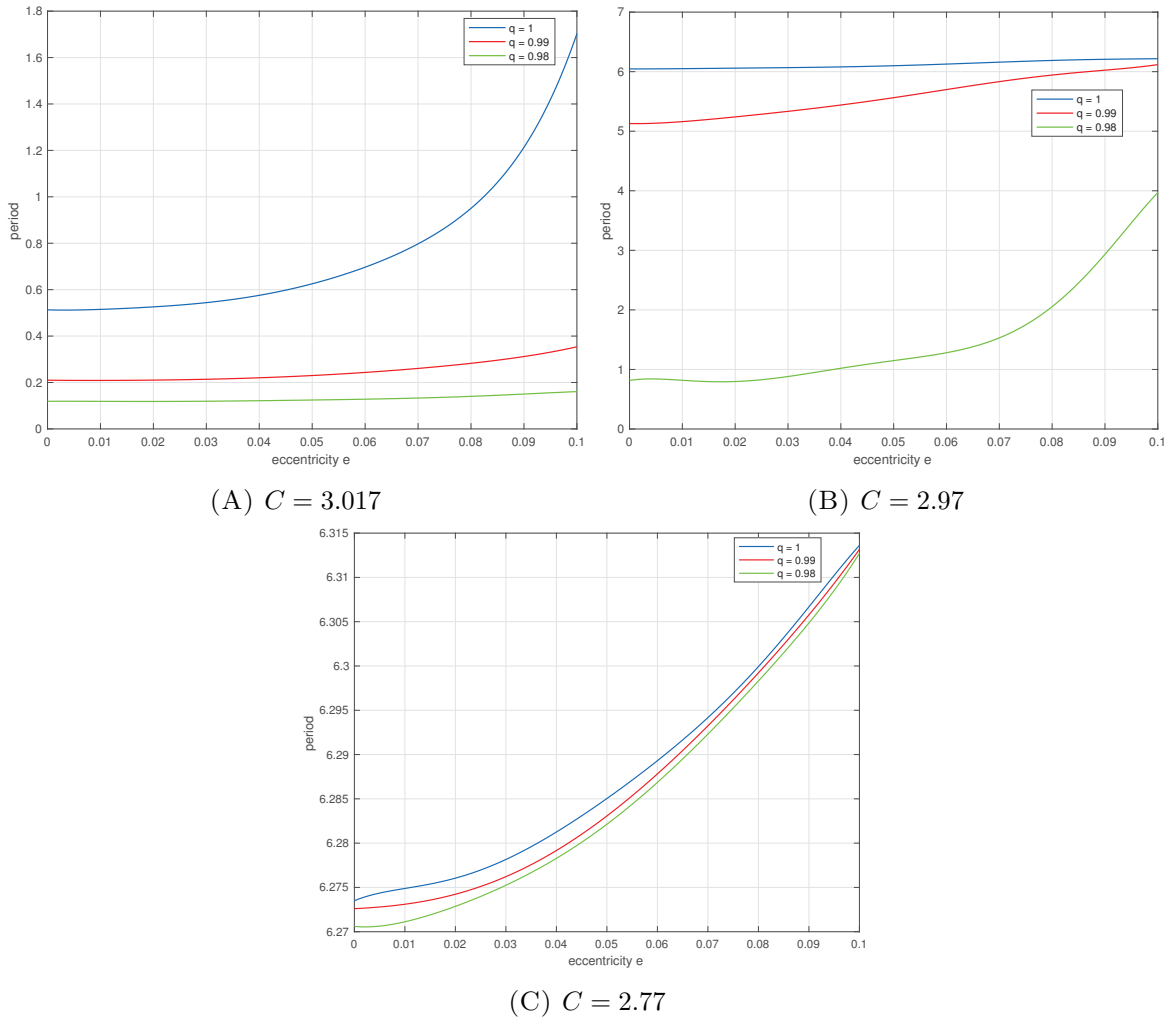


FIGURE 5.8: Variation in period of orbits due to variation in radiation pressure

When $C = 2.77$, no sudden change in the location of orbits is observed (Fig. 5.3(C)). So, the locations of periodic orbits depend on the radiation pressure and energy level also. f -family orbits move towards the second primary P_2 with the increase in radiation pressure of the first primary P_1 .

The effect of perturbation due to radiation of the first primary on diameter of f -family orbits is shown in Fig. 5.4 for $C = 3.017, 2.97$ and 2.77 . In Figs. 5.4(A), 5.4(B) and 5.4(C), the curves in blue, red and green correspond to $q = 1.00, 0.99$ and 0.98 , respectively. The diameter of orbit decreases due to increase in solar radiation pressure. The functional relation between diameter and e is different for different values of q and C . For $C = 3.017$, a sudden increase in diameter is observed for $e \geq 0.045$ (Fig. 5.4(A)) when the perturbation of solar radiation is neglected while no such sudden change is observed for $q = 0.99$ and 0.98 . In Fig. 5.4(B), a sudden change in diameter is observed for $q = 0.98$ whereas in Fig. 5.4(C), no sudden change in d is observed. From Fig. 5.4,

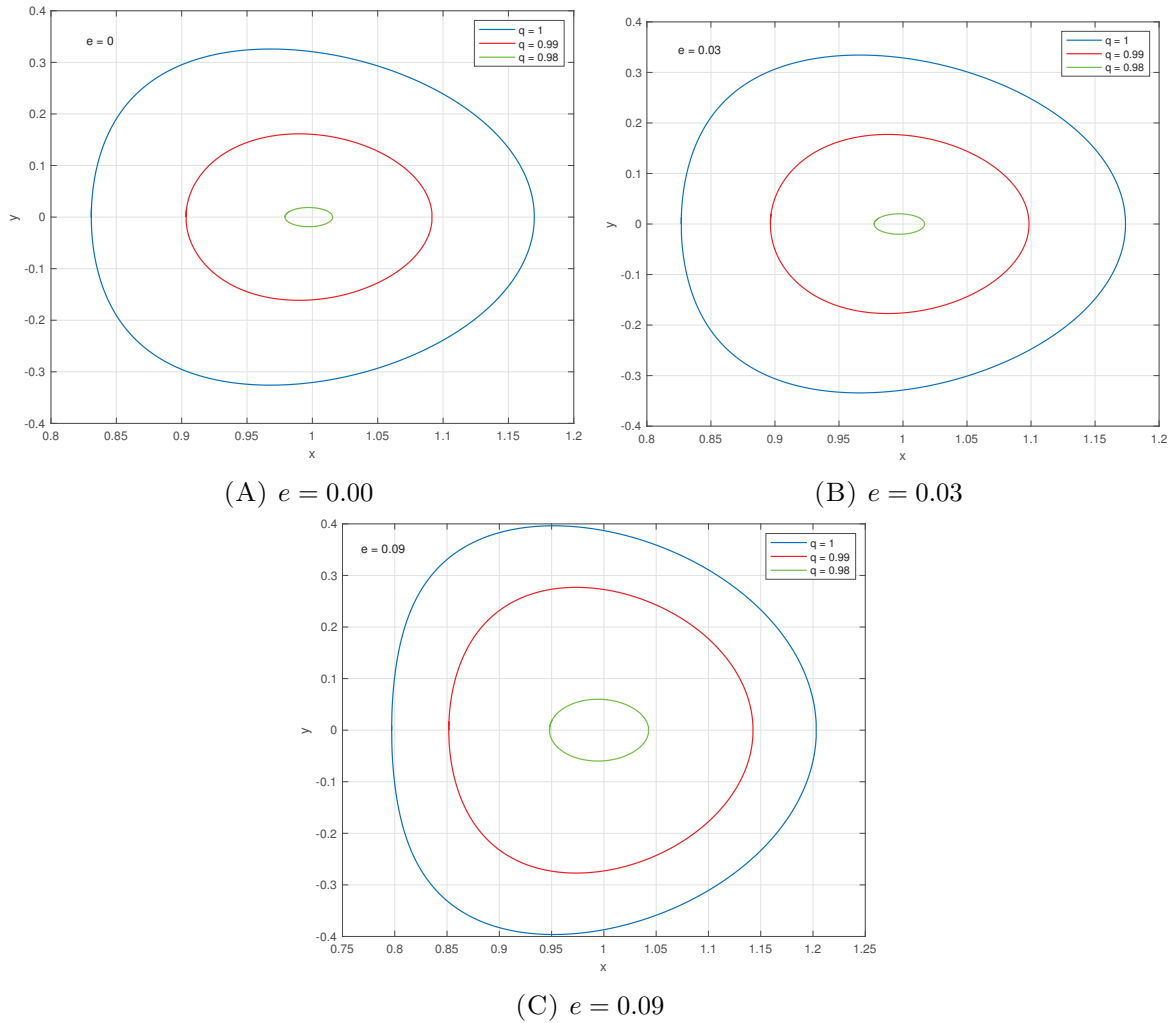


FIGURE 5.9: Variation in shape and size of orbits due to variation in radiation pressure for $C = 2.97$

it can be concluded that due to radiation pressure of the primary, orbits shrink.

The change in size and shape of f -family orbits due to radiation pressure is shown in Fig. 5.9. In Fig. 5.9(A), 5.9(B) and 5.9(C), three different values for e are considered to study the effect of q on size and shape of orbits. In the absence of radiation pressure, the shape of orbits is like an egg. As radiation pressure increases, orbits become elliptical and they shrink.

The change in the shape and size of the islands due to solar radiation pressure are shown in Fig. 5.10. As solar radiation pressure increases, island becomes like a triangle and move towards the second primary.

As shown in Fig. 5.6, for $e = 0$, the difference $C_2 - C_1 = 0.0062$ when $q = 1$ and

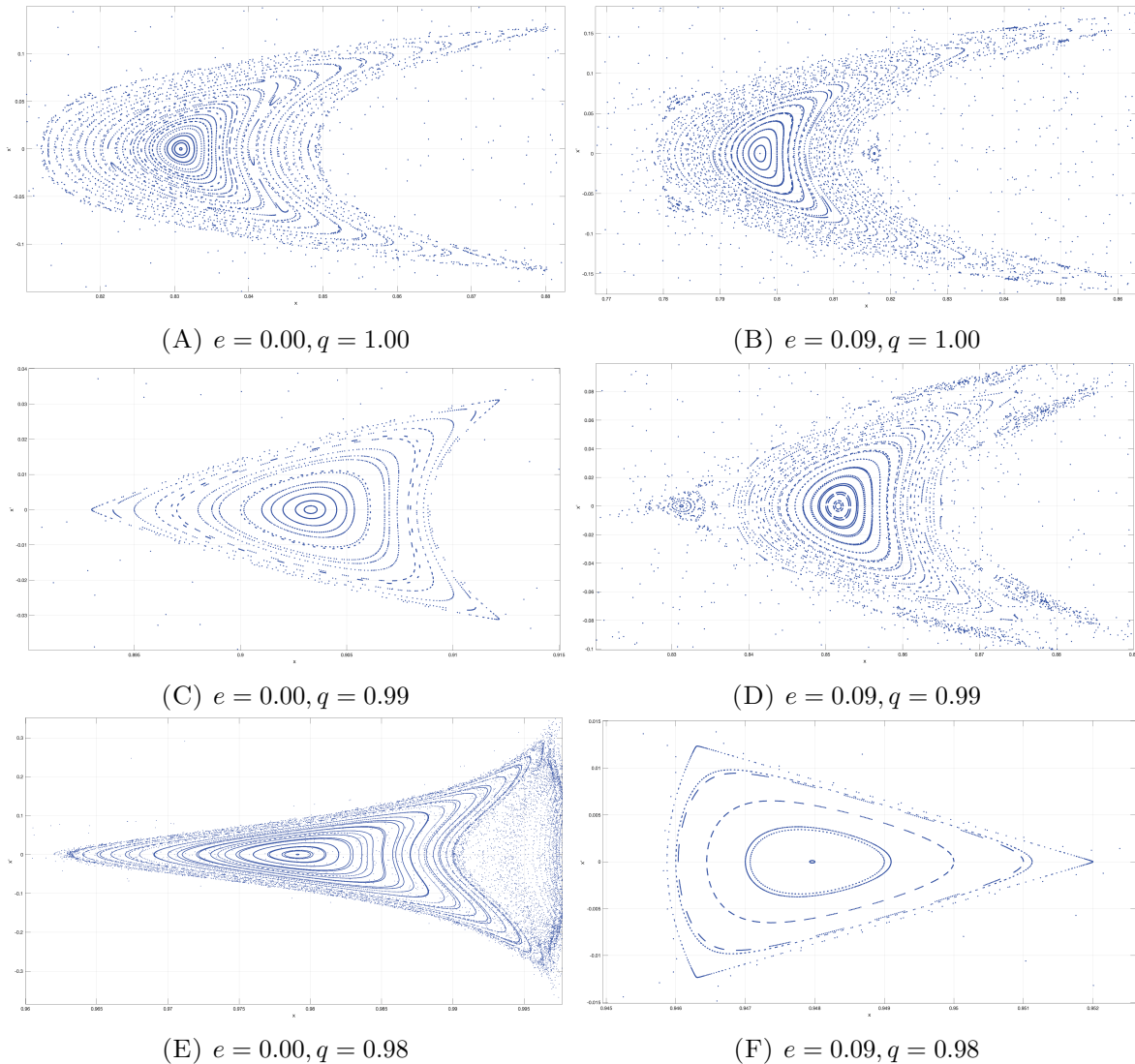


FIGURE 5.10: Variation in shape and size of islands due to variation in radiation pressure for $C = 2.97$

$C_2 - C_1 = 0.0063$ for $q = 0.98$. Also, for $e = 0.09$, $C_2 - C_1 = 0.0062$ when $q = 1$ and $C_2 - C_1 = 0.00662$ when $q = 0.98$. This shows the difference between the energy levels at separatrices increases due to increase in radiation pressure. It is further noted that the value of C at separatrices decreases due to perturbation of radiation pressure.

In Fig. 5.8, changes in the values of period of f -family orbits are shown graphically. The curves corresponding to $q = 1.00, 0.99$ and 0.98 are shown in blue, red and green colours, respectively. In Fig. 5.8(A), a sudden increase in period can be observed for $q = 1$ while in Fig. 5.8(B), for $q = 0.98$ a sudden increase in period is observed. It can be concluded that periods of orbits decrease due to increase in solar radiation pressure (Fig. 5.8).

5.4.3 Effects of Jacobi constant

The energy constant, also known as the Jacobi constant, C , is an important factor in determining the size of excluded regions, the orbital parameters and the position of periodic orbits. Table 5.1 shows as C increases, the excluded region enlarges and shifts towards the first primary.

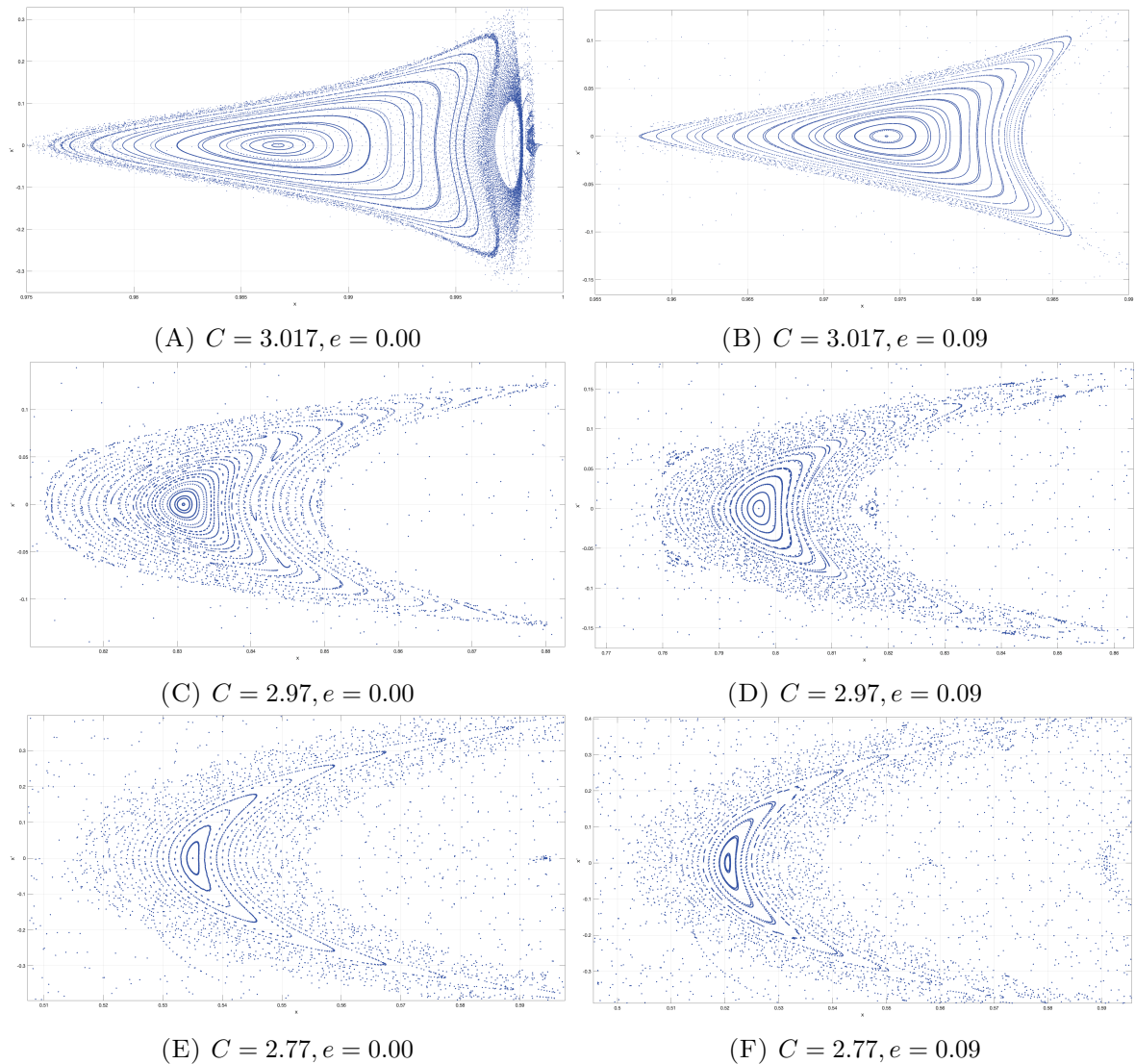


FIGURE 5.11: Variation in shape and size of islands due to variation in energy constant C for $q = 1$

Fig. 5.3 illustrates how the location of f -family orbits vary for $C = 3.017, 2.97$ and 2.77 . It indicates that orbits get closer to the second primary with the increase in the value of Jacobi constant. Fig. 5.4 shows that the diameter of the orbits decrease due to increase in the value of Jacobi constant. Similar effect of Jacobi constant on period of f -family orbits is observed (Fig. 5.8). The value of C also affects the

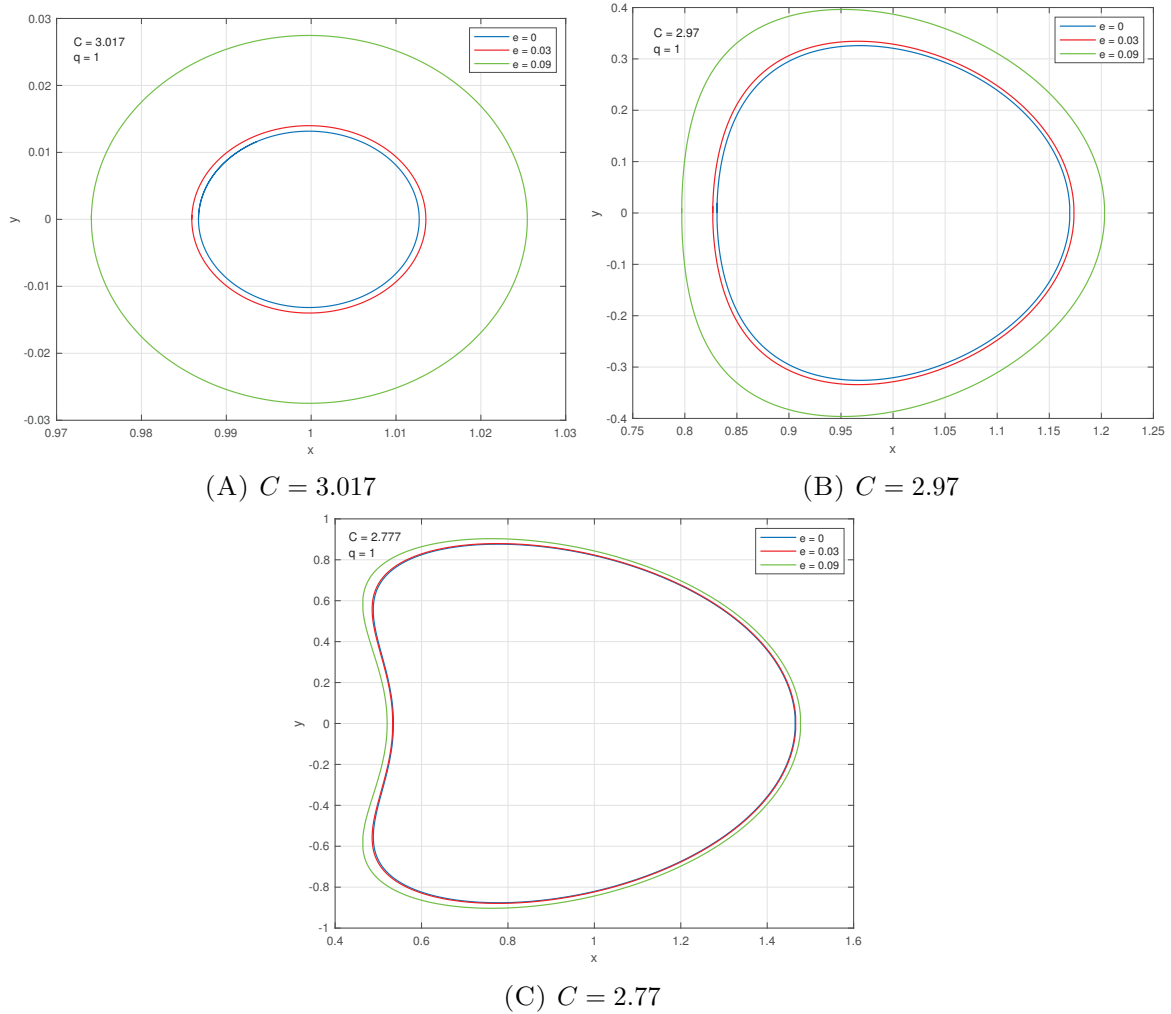


FIGURE 5.12: Variation in shape and size of orbits due to variation in energy constant for $q = 1$

functional relationships between orbital parameters of f -family orbits and eccentricity (e) of primaries.

The f -family orbits for $C = 3.017$ are elliptic and for $C = 2.97$, their shape is like an egg. If C is decreased further, say, $C = 2.77$, then these orbits no longer remain elliptic or egg shaped. f -family orbits for three different values of C are given in Fig. 5.12. Also, the orbits expand in size as the value of C decreases. This agrees with the conclusions of Fig. 5.4. In all numerical calculations, the value of $e = 0$ corresponds to CRTBP and $q = 1$ means there is no perturbation due to solar radiation pressure.

5.5 Conclusions

In this chapter, the motion of an infinitesimal body is considered in ERTBP framework with eccentric anomaly as independent variable. The equations of motion of the

infinitesimal body are averaged with respect to the independent variable, eccentric anomaly, in order to get autonomous system of equations which provides the existence of integral of motion/ Jacobi constant. By extending the method of Poincaré Surface of Sections from CRTBP to ERTBP framework, the islands containing *f*-family orbits in the Sun-Saturn system are obtained. The Sun is considered as a source of radiation. The effects of eccentricity of orbit of primaries, solar radiation pressure and Jacobi constant on shape and location of islands and parameters of *f*-family orbits are investigated.

The investigation shows that due to non-zero value of eccentricity of primaries' orbit, the size and shape of islands containing *f*-family orbits change. Further, these islands shift near the Sun as the value of e increases. The analysis shows that the maximum permissible value of Jacobi constant increases and the excluded region for $C > C_M$ contracts due to increase in the eccentricity of primaries' orbit. Further, these orbits expand and their periods increase as the value of e increases. The functional relation between parameters of *f*-family orbits and e is monotonic and non-linear.

The study of effects of solar radiation shows that with the increase in solar radiation pressure, island becomes like a triangle and shifts towards the Saturn. Further, with the increase in solar radiation pressure, the maximum permissible value of Jacobi constant decreases while the excluded region expands. The orbits shrink, so their diameter and period decreases as the solar radiation pressure rises. The value of Jacobi constant at which separatrix occur also depends on the value of solar radiation pressure.

From the analysis, it is observed that the values of parameters of *f*-family orbits depend on the value of Jacobi constant also. The shape of islands containing *f*-family orbits change and they shift towards the Saturn as Jacobi constant increases. Further, the orbits shrink and hence the diameter and period decreases as C increases.

So, we can conclude that the eccentricity of primaries' orbit, solar radiation pressure and the value of Jacobi constant affects all parameters of *f*-family orbits. Further, the eccentricity and solar radiation of primaries play an important role in the determination of location and length of excluded region.